Obstacle marks as palaeohydraulic indicators of Pleistocene megafloods

Jürgen Herget, Thomas Euler, Thomas Roggenkamp and Julian Zemke

ABSTRACT

Pleistocene megafloods generated several large-scale obstacle marks that could not be interpreted hydraulically with the present knowledge of submerged obstacles. Thus, flume and field data of classical obstacle marks, characterised by a frontal scour hole and an adjacent depositional ridge, are analysed to estimate flow velocities from obstacle mark geometry, especially scour depths, length, width and ridge width. These data reveal a consistency of correlations between obstacle mark morphometries across a wide spatial scale. Two existing analytical models, basically integrating obstacle size, flow velocity as well as sediment size and grading, are transformed so that the magnitude of individual geometric parameters can be used as variables for the estimation of mean and tip flow velocities. These reconstructed velocities have to be regarded as minimum velocities during the rising limb of the hydrograph, as peak discharge might not last long enough to significantly influence the obstacle mark dimensions. A universally applicable practical outline is developed for palaeohydraulic reconstruction. This framework is applied on three examples of obstacle marks generated by Pleistocene megafloods. The reliability and scale-invariance of these reconstructions is confirmed by similar results of velocity estimations by other independent approaches at the same locations.

Key words | local scour, obstacle mark, outburst flood, palaeoflood reconstruction, palaeohydrology, sedimentary structure

Jürgen Herget (corresponding author)
Thomas Euler
Thomas Roggenkamp
Department of Geography,
Bonn University,
Meckenheimer Allee 166,
53115 Bonn,
Germany
E-mail: *herget@giub.uni-bonn.de*

Julian Zemke
Institut für Integrierte Naturwissenschaften,
Abteilung Geographie,
Koblenz University,
Universitätsstrasse 1,
56070 Koblenz,
Germany

INTRODUCTION

The extended glaciations during the last Ice Age generated large ice-dammed lakes in many glaciated areas of the world. Instabilities in the ice dams, especially during the decay of the ice shields and mountain glaciers after about 20 ka BP resulted in high magnitude outburst floods, called jökulhlaups, after the term for such events in Iceland. These outburst floods were obviously much larger than any recent flood event on Earth, indicated by peak discharges of millions of cubic metres per second (O'Connor *et al.* 2002). Such 'superfloods' (Baker 2002) caused significant and complete changes in the entire landscape along their pathways due to the eroded bedrock and reworked sediments and therefore are characterised as cataclysmic (Baker 1988).

Prominent examples for such Pleistocene megafloods with discharges of $>10^6$ m³/s are those from glacial Lake Missoula in northwestern USA (e.g., Baker 2009; Denlinger & O'Connell 2010), where a lobe of the Cordilleran ice sheet blocked the course of Clark Fork River and generated an ice-dammed lake in western Montana. The repeated outburst floods inundated most parts of eastern Washington and eroded the Channelled Scabland, and consisted of numerous floods hundreds of metres deep that eroded wide channels into the bedrock before reaching the Pacific Ocean via the Columbia River valley.

A similar event took place in the Altai Mountains, south-central Siberia around the same time (Herget 2005; Carling *et al.* 2010). Valley glaciers in the nowadays partly semi-arid mountain range advanced and blocked the course of the River Chuya, located in the headwaters of the River Ob near the border with Mongolia. The repeated outburst

doi: 10.2166/nh.2012.155

floods were channelled through the mountain valleys instead of incising new flood channels and faded out in the vast extension of the East Siberian Plain.

The drainage of Lake Agassiz, located in varying extensions of the southern part of the remnants of the Laurentian ice sheet at the end of the last glaciation until early Holocene times (Teller 2004; Kehew *et al.* 2009), influenced global climate conditions. The large volume of released water influenced ocean currents, especially the thermohaline circulation, resulting in temporary cold reversals at 8.2 ka BP and initiating the Younger Dryas cold event in the Late Glacial (e.g., Clarke *et al.* 2004; Murton *et al.* 2010; Rayburn *et al.* 2011). In addition to the outburst floods, spillways from Lake Agassiz and its predecessors directed lake water into the drainage systems of the Mackenzie River towards the Arctic, via the St Lawrence and Hudson rivers into the Atlantic and via the Mississippi River into the Gulf of Mexico. It is assumed to have been involved in the initiation of temporary climate changes towards warmer conditions (e.g., Erlingsson 2008).

For the hydrologist, the magnitudes of the outburst floods, best characterised by peak discharge, are even more interesting than the slightly differing impressive flood environments of the Pleistocene megafloods. Discharge estimations are principally based on the continuity equation $Q = Av$ with cross-section area A and mean flow velocity v as unknown variables. Based on palaeostage indicators of flood level, e.g., the surface of gravel bars or slack water deposits (Jarrett & England 2002), the cross-section area of the discharge in a valley can easily be quantified. More challenging is the estimation of the flow velocity. Approaches based on slope, channel geometry and hydraulic roughness, like the well-established Manning equation for the mean flow velocity $v = R^{2/3}\ S^{1/2}\ n^{-1}$ (R – hydraulic radius, S – slope of the energy line, n – empirical hydraulic roughness coefficient) (Chow 1959), are most frequently applied. Starting with simple one-dimensional steady flow approaches based on single profiles, software-supported gradually varying unsteady flow conditions along valleys can be modelled by the Hydrologic Engineering Center's River Analysis System (HEC-RAS) (Brunner 2010). This approach was applied for the outburst floods from Lake Missoula (O'Connor & Baker 1992; Benito 1997), for floods in the Altai Mountains (Baker *et al.* 1993; Herget 2005; Rudoy & Zemtsov 2010) and in a comparable way for Holocene events in Iceland (e.g., Alho *et al.* 2005, 2007; Howard *et al.* 2011). Subglacial outburst floods originating from Lake Agassiz were estimated from physically based modelling considering parameters such as water temperature, density of water and ice or inflow into the lake, which are critically discussed and analysed (Clarke *et al.* 2004). Also for the other examples mentioned above, more advanced and sophisticated models are applied, considering two-dimensional flow conditions, dam failure processes and duration, or replacements of deposits from previous outburst floods (e.g., Clarke *et al.* 1984; Miyamoto *et al.* 2007; Alho *et al.* 2010; Carling *et al.* 2010; Denlinger & O'Connell 2010). Principally, the more advanced models confirm the magnitude of previous findings even if the more simplistic approaches are less realistic. Therefore, Carling *et al.* (2003) concluded that the required estimations and assumptions with their problematic validation are frequently out of balance considering input and findings. Furthermore, the technical challenge even to handle the more complex expert models might not be well balanced with the increase in dependable gain of knowledge.

Hydraulic interpretations of sedimentological and geomorphological structures of high magnitude megafloods are rather rare. The main reason is the problematic extrapolation of findings and relations from the well-studied ordinary smaller scale of forms, grain sizes, depths of flow and flow velocities to high magnitude conditions.

The problem can be illustrated by the competence approach relating grain size of transported sediments during a flood event to flow velocity. The transformation of shear stress of the current to mean flow velocity works rather well for small grain sizes up to about 33 cm mean diameter (Zanke 1982) and shallow flow conditions (Baker 1973). The extrapolation towards coarser grain sizes leads to a systematic overestimation of the required flow velocity for their transport, which is characterised as typical for the extrapolation of several physically based relations (Komar 1989). Costa (1983) developed an empirical relationship for this background for deposits up to a mean diameter of 3 m, but recognised significant scattering of the data around the regression equation for large grain sizes. The increasing range of required flow velocities for boulder transport can be explained by macroturbulence effects (e.g., Matthes 1947; Baker 1973) resulting in an overproportional

increased lift-force by vortices around the particle compared with smaller grain sizes. Obviously, this phenomenon depends on the shape of the transported particles and therefore the scatter of related mean flow velocity increases significantly.

Bedforms on the channel bottom are studied intensively for their formation, sedimentology and structure (e.g., Allen 1968, 1984; Leeder 1999; Bridge 2003), but rarely have been interpreted quantitatively for hydraulic conditions during their generation, especially for megafloods. One example is the interpretation of fluvial gravel dunes found at several locations in the Altai Mountains by Carling (1996a, 1996b, 1999). In contrast to previous interpretations, he could show that the large gravel dunes with heights up to 16 m were formed under relatively shallow flow conditions and are not related to peak discharge of the outburst floods draining the lake.

Obstacle marks were studied by the examples of stranded ice-blocks deposited during recent jökuhlaups in Iceland (e.g., Fay 2002; Carrivick *et al.* 2004; Russell *et al.* 2006). Pleistocene large-scale features in the basins and valley bottoms have also been observed along the pathways of the Pleistocene outburst floods related to Lake Missoula and in the Altai Mountains. Beyond descriptions, no further interpretations have been undertaken. First approaches based on rule-of-thumb from engineering references failed, as depths of flow in relation to the dimension of the form would lead to a spill over of the lake water above the neighbouring mountain ranges (Herget 2005).

Consequently, more systematic research, including flume experiments, focusing on submerged obstacles, was undertaken for a better understanding of the processes and dynamics involved. The aim was investigate the value of obstacle marks as palaeohydraulic indicators. Therefore, in a first step, the dominating factors of obstacle, current and sedimentary conditions for the obstacle mark's geometry are determined. Next, the transformation of existing analytical models is carried out to use preserved obstacle marks for the reconstruction of flow velocities during their formation. Based on these findings summarised in review in the following section, a practical outline for palaeohydraulic interpretation of obstacle marks is presented and applied on selected examples of local scour structures related to Lake Missoula and Altai Mountains jökulhlaups. In the final discussion, perspectives and limitations of the approach are discussed.

PROCESSES AND DYNAMICS OF OBSTACLE MARK FORMATION

Obstacle marks are sedimentary structures induced by in-stream obstacles located on the channel bed (Figure 1). Such obstacles force the flow to locally separate resulting in a three-dimensional turbulent flow field around the obstacle (Figure 2). This hydraulic process leads to local erosion around the obstacle and re-deposition of sediments in its wake. The spatial pattern of the sediment redistribution is typically characterised by a frontal, crescent-shaped scour hole and a leewise depositional sediment accumulation, denoted as a 'sediment ridge'. In the case of fluvial obstacle marks, hydraulic and sedimentary processes exist in a strong dynamic interaction, resulting in non-linear form development (Melville & Coleman 2000; Euler &

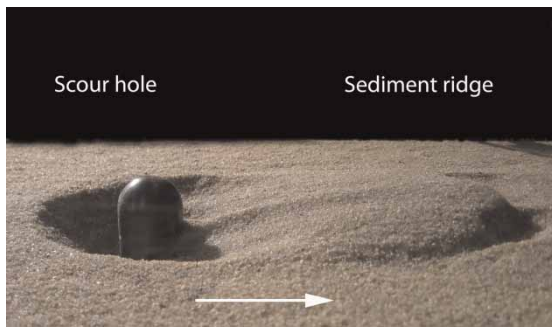

Figure 1 | Photo of a typical obstacle mark in a flume with a frontal scour hole and a reposition of the eroded sediments in the wake of the obstacle. Diameter of the obstacle is 3.0 cm.

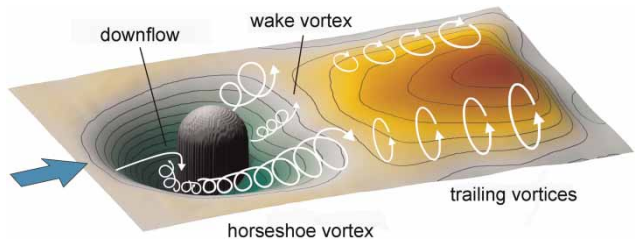

Figure 2 | Three-dimensional turbulent flow field around a submerged obstacle with frontal scour hole and accumulated sediment ridge in the wake. Direction of flow is left to right. Note that for clarity only the right side of the symmetric vortex system is illustrated.

Herget 2011, 2012). In the initial phase of obstacle mark formation, the approaching currents are pushed down in front of the obstacle and get accelerated at the lateral parts. This downflow erodes an initial small scour hole in front of the obstacle. Furthermore, the down flowing currents are redirected into the upstream direction at the frontal base of the obstacle so that a rotating vortex system develops. Because this vortex system extends around the obstacle base in a horseshoe-like pattern, it is denoted as a 'horseshoe vortex'. The horseshoe vortex is mainly responsible for the following local scouring process and the most dominant feature of obstacle mark systems. In fact, scour hole incision and horseshoe vortex action promote a positive feedback loop up to the point where the scour hole has reached a critical size so that the erosive potential of the horseshoe vortex is reduced. The scour hole then approaches a steady-state condition, dominated by a negative feedback loop. Its slopes basically follow the angle of repose of the sediment. Apparently, the change from positive to negative feedback loop is the cause for the non-linearity of obstacle mark morphodynamics. Figure 3 displays an exemplary non-linear scour hole incision during a laboratory flume experiment.

Leewise of the obstacle, two major hydraulic processes govern the local sediment flux (Figure 2). First, the legs of the horseshoe vortex are extending in a downstream direction on each side of the obstacle and thus transport the scoured material out of the scour hole into the wake region of the obstacle. Second, laterally detaching shear layers generate an unsteady counter-rotating vortex system that, to a great extent, shapes the sediment ridge topography. In addition to that, both horseshoe vortex legs and detached shear layers interact at some distance behind the obstacle and lead to the generation of 'trailing vortices'. These can continue far downstream and have the potential to create sediment ridges with lengths up to several tenths of the obstacle diameter.

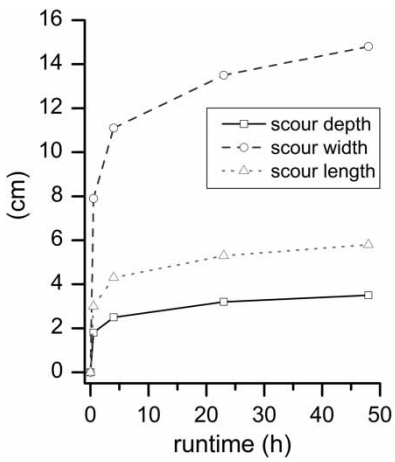

Figure 3 | Non-linear development of scour hole morphometry during own flume experiments. The obstacle is a cylinder with a diameter of 3.0 cm and a height of 2.5 cm above plane bed. For the experiment, the cylinder was embedded in uniform coarse sand ($D_{50} = 0.75$ mm) and exposed to steady water flow for 48 hours with a mean velocity of 24.3 cm/s and a water depth of 6.5 cm.

However, if, under given boundary conditions, the downflow in front of the obstacle is not strong enough to erode an initial scour hole, the system changes into a completely different state. This can be, for example, the case when the frontal obstacle area is strongly inclined into the streamwise direction. For emergent cylinders, Zemke (2011) experimentally determined a critical cylinder inclination of 20–30°. The horseshoe vortex then remains very small and does not play a significant role in further form generation. Instead, wake vortices and the detaching shear layers create a zone of current recirculation in the obstacle wake, as commonly known from flat bed fluid mechanical studies (e.g., Sadeque *et al*. 2008). Under these conditions, the currents, which are separated at the obstacle, reattach to the bed behind the obstacle and hence cause leewise instead of frontal scouring. The total sediment flux in this state, however, is much smaller than under the presence of a fully developed horseshoe vortex. Figure 2 highlights both described system states with respect to steady-state topographies and the prevailing hydraulic processes.

Given that it may be impractical to measure detailed obstacle mark topographies in the field and that obstacle marks are often imperfectly preserved, several morphometric variables were determined from flume experiments and a field study (Euler 2012) for simplistic representation of obstacle mark topographies. These include: maximum scour depth (d_s); width of the frontal scour hole (w_s); length of the frontal scour hole (l_s) at the plane of symmetry and maximum width of the sediment ridge (w_r). The unique characteristic of these variables is that they stand in a significant linear relationship to each other, so that the precise knowledge of one of these variables enables an estimate of the others, as Figure 4 highlights. Due to the very good correlations, a potential scour depth for steady-state conditions

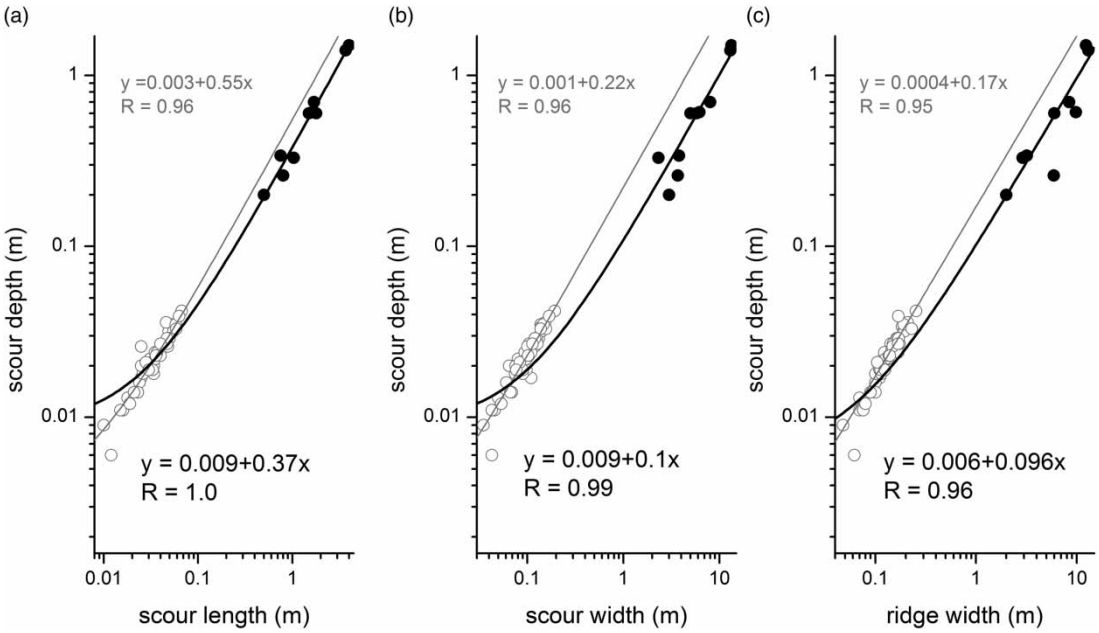

Figure 4 | Linear regression functions for potential scour depth estimation. The functions in grey were calculated from laboratory data only, while the functions in black were calculated from both laboratory and field data. Laboratory data (grey open circles) result from own experiments with submerged obstacles in a hydraulic flume, with scour depths: 0.006–0.042 m; scour lengths: 0.01–0.067 m; scour widths: 0.035–0.194 m; and ridge widths: 0.048–0.255 m. Field data (black filled dots) result from own surveys of recent obstacle marks in two Spanish ephemeral streams (Euler 2012), with scour depths: 0.2–1.5 m; scour lengths: 0.5–4.0 m; scour widths: 2.33–13.4 m; and ridge widths: 2.0–13.0 m. Only fully developed obstacle marks were considered.

can be estimated. Note that especially for large-scale obstacle marks this maximum value might not be preserved, as the main process for frontal scour hole enlargement is sliding due to gravity and the angle of response related to grain size of the sediments (Euler & Herget 2011, 2012). During the final stage of a flood, the downflow and resulting horseshoe vortex system might not be strong enough to remove sediments sliding into the frontal scour hole, especially for overdeepened holes of tenths of metres. In contrast to the obstacle mark geometry parameters mentioned above, the variables 'sediment ridge length' and 'height' are not suited for correlations, as they strongly vary with time and frequently do not reach steady states (Euler 2012).

In general, critical thresholds for obstacle mark formation and obstacle mark sizes are controlled by a variety of independent variables. The most important variables in this context include: width and height of the projected frontal area of the obstacle, obstacle shape, sediment size, mean flow velocity and water depth. As well, the duration of steady flow, unsteady flow effects (i.e., flood wave action or pulsating flow), the impact of incoming sediments from mobile bedforms and obstacle movability (i.e., obstacle anchorage and geometry) also play a role in obstacle mark generation. Most of these variables have been incorporated into appropriate analytical models (Euler & Herget 2011, 2012) that aim to determine corresponding steady-state dependent variables (such as scour depth) satisfactorily. The models were developed from laboratory studies and have been validated with independent laboratory and field data. In their non-dimensional form they are written as:

$$\log_{10}\left(\frac{d_s}{\left(\frac{\nu}{U_m}\right)}\right)^{1/2} = 0.25 + 0.5\log_{10}\left(Re_o Fr^{1/2} K_{sed}\right) \quad (1)$$

$$\log_{10}\left(\frac{d_s}{\left(\frac{\nu}{U_t}\right)}\right)^{1/2} = 0.27 + 0.46\log_{10}(Re_{Po}) \quad (2)$$

with $K_{sed} = K_{D50}K_\sigma$, where $K_\sigma = 1/\sigma_g$ and $K_{D50} = 1/(1 + (-0.050(w_o/D_{50}) + 2.5))$, if $w_o/D_{50} < 50$, or $K_{D50} = 1/(1 +$

$(0.0003(w_o/D_{50}) - 0.01))$, if $w_o/D_{50} > 50$; Re_o = obstacle Reynolds number $((U_m\ L_A)/\nu)$, Re_{Po} = potential obstacle Reynolds number $(((U_t\ D_{equ})/\nu)\ K_{sed})$, Fr = Froude number $(U_m/(d_w\ g)^{1/2})$, U_m = mean flow velocity, U_t = tip-velocity, L_A = equivalent length of projected frontal area $(h_o^{2/3}\ w_o^{1/3})$, D_{equ} = equivalent diameter of projected frontal area $(2((h_o\ w_o)/\pi)^{1/2})$, w_o = obstacle width (note comment below), h_o = obstacle height (note comment below), D_{50} = median of the grain size distribution, σ_g = geometric standard deviation of the grain size distribution $((D_{84}/D_{16})^{1/2})$, g = gravitational acceleration, d_w = water depth, ν = kinematic viscosity and d_s = frontal scour depth. 'Tip-velocity' denotes the velocity approaching the obstacle at its highest elevation. Recently, Euler (2012) suggested a simplified procedure to also account for different obstacle shapes (Table 1): thereby, obstacle height h_o is multiplied with 0.85, if the vertical profile of the projected frontal has a streamlined shape. When the obstacle is rectangular or elliptically shaped in the planview, obstacle width w_o is multiplied with 1.1 or 0.8, respectively.

It is evident from Equations (1) and (2) that the models are mainly based on obstacle Reynolds number, which expresses the relation between turbulent and viscous forces in the vicinity of the obstacle (Euler & Herget 2011), and furthermore include empirical correction factors for sediment size and non-uniformity. While in the first model (Equation (1)) 'mean flow velocity' and 'water depth' are the independent variables for flow characterisation, the second model (Equation (2)) incorporates the variable 'tip velocity' for this purpose only.

Table 1 | Correction factors for obstacle width and height depending on the obstacle's shape

width	height
1.0	0.85
0.8	1.0
1.1	

The analytical models are valid for both submerged and emergent obstacles, but do not account for the presence of very large mobile bedforms, such as ripples or dunes. However, as long as the bedform height is lower than the obstacle height, the horseshoe vortex can cope with the periodically increased sediment input into the scour hole and scour depth values will oscillate around the maximum potential clear-water value (cf. Melville & Coleman 2000).

FRAMEWORK FOR PALAEOHYDRAULIC RECONSTRUCTION OF FLOW VELOCITY

To make use of fluvial obstacle marks as palaeohydraulic indicators, a procedural framework consisting of seven steps is suggested. These steps comprise:

1. Survey of the obstacle mark morphometry;
2. Survey of obstacle geometry;
3. Investigation of the locally reworked sediments;
4. Estimation of hydraulic boundary conditions by other indicators;
5. Evaluation of uncertainties like duration of obstacle mark generation, unsteady flow, sediment replacement;
6. Iterative application of the analytical model to estimate flow velocity;
7. Plausibility tests.

In the following text, each of these steps will be outlined in more detail.

To collect the dependent key variables needed for reconstruction, – scour-width, -length and -depth and sediment ridge width as well as (if possible) eroded and deposited volume – surveys have to be conducted. If this is not possible, remote sensing of the obstacle mark size and geometry may be performed using air photographs, topographic maps or digital elevation models, depending on the size of the feature. In case of sediment infills in the scour hole, which leads to a reduction of scour depth, analysis of the stratigraphic record (see Underwood & Lambert 1974) should additionally be carried out, for example by core-sampling or indirect methods such as geoelectric and seismic ground penetration.

However, as this may not always be possible under the given boundary conditions at the sites, an estimation of

the steady-state scour depth can be derived from data of scour hole width and frontal length as well as from sediment ridge width. These variables are usually well preserved and remain constant even when sediment from smaller floods or during the waning stage of a megaflood was deposited in the scour hole. Hence, the three linear functions

$$d_s = 0.009 + 0.1w_s \quad (3)$$

$$d_s = 0.009 + 0.37l_s \quad (4)$$

$$d_s = 0.006 + 0.096w_r \quad (5)$$

as displayed in Figure 4 can be applied for this purpose (all parameters in metres). For geometric reasons, there might be only minor derivations from these functions due to differences in the angle of repose of the sediment, depending on its dominant grain size. The application of Equations (3), (4) and (5) allows estimations, whether the scour hole's formation reached steady-state conditions or was hindered in its development. Limitation could be caused, e.g., by relatively thin sedimentary layers resulting in only an initial development of the frontal scour depth by significantly more resistant bedrock layers below.

In addition, horizontal knickpoints in the ridge or superimposed ridges with different orientations and sedimentary compositions may provide information about differing flow directions during formation (e.g., Nakayama *et al*. 2002).

Of central importance for the reconstruction is knowledge about the height and width of the projected frontal area and its streamwise inclination. The horseshoe vortex strength reduces with decreasing size and increasing inclination of the projected frontal area. The appropriate values can be estimated in a similar manner as outlined above, whether based on surveyed field data or by remote survey techniques.

Additionally, it should be known, whether the obstacle is anchored, such as rocks, or moveable, such as boulders. In the case of moveable obstacles, obstacle length in the streamwise direction in combination with scour depth indicates whether the obstacle has tilted into the scour hole or not. Tilting occurs if a critical frontal scour depth is exceeded so that the obstacle tilts upstream due to its weight distribution (Fahnestock & Haushild 1962; Sengupta 1966; Euler 2012). For an evenly shaped and well-balanced obstacle such as a sphere, the appropriate threshold for tilting was experimentally found to be $d_s = 0.6\ l_o$, with $l_o =$ obstacle length in the streamwise direction (Euler 2012). Generally, when an obstacle tilts into the scour hole, steady-state conditions are reached quickly, for the projected frontal area and hence the erosive strength of the horseshoe vortex suddenly decreases. At this point it has to be noted that the dropping obstacle might rotate depending on its weight and geometry. For palaeoflow reconstruction, the preserved projected frontal area should be used as independent variable.

Ideally, information on the median (D_{50}) and the geometric standard deviation (σ_g) of the grain size distribution upstream of the scour hole is given for the analytical models. These values can be determined by bulk-sampling of the sediments on-site. If bulk-sampling is not possible, the three axes of the largest grains should be measured manually, so that their mean value can be used instead of D_{50} and σ_g. The mean value D_{50} then approximates the largest particle sizes of the grain size distribution, such as D_{84} or D_{90} (cf. Lai *et al*. 2009), consequently $D_{50} = D_{84}$ and $\sigma_g = 1$ are assumed. Although this procedure will lead to a slightly reduced accuracy of the velocity calculations, the overall error remains within the expected ranges of uncertainties.

For correct determination of obstacle height, it should be known if the obstacle was submerged during the peak flood stage or not. Approximate knowledge on water depth is furthermore important for correct application of Equation (1), as current conditions expressed by Froude number depend on depth of flow. This also applies for water temperature, because kinematic viscosity is an integral element of the analytical models. Here, merely rough estimations are sufficient (such as kinematic viscosity for 4, 10 or 20° C) as values for water temperature cannot be verified.

Eventually, the modeller has to know, if for the given boundary conditions, bed shear stresses were above the critical values for general sediment transport during the flood event. Preserved dunes or ripples might indicate such lifebed conditions. However, if the height of these moving bedforms is larger than the obstacle height, the obstacle mark

may have been completely buried. Flow reconstruction will be difficult under these conditions. On the other hand, if bedform height is lower than obstacle height, the present scour depth can be equated with maximum scour depth as differentiations between life-bed or clear-water conditions are not considered in the models.

The most significant source of uncertainty involved in this modelling approach is the effect of unsteady flow. As the analytical models refer to steady-state conditions, the reconstructed flow velocities have to be regarded as minimum velocities during the rising limb of the hydrograph, because peak discharge might be assumed to not last long enough (e.g., >4–5 h, Figure 3) to significantly influence the obstacle mark dimensions. The falling limb of a hydrograph generally has little effect on scour hole morphometry (Chang *et al*. 2004; Oliveto & Hager 2005; Euler 2012). With respect to uncertainties due to (post-flood) sediment infill in the scour hole, badly preserved forms or unknown boundary conditions, possible scenarios are considered as ranges of uncertainty in a quantitative sense for different parameters.

Finally, if all necessary data are gathered and evaluated, the analytical models (Equations (1) and (2)) can be applied iteratively for calculations of mean and tip flow velocities. However, the disadvantage here is that on the one hand flow velocities appear on both sides of Equations (1) and (2), and that on the other hand both equations rely on empirical correction factors for sediment size, which were only tested for a limited spatial range (see Lee & Sturm 2009). A second possibility is to solve the original functional relationships by mean and tip flow velocity, respectively, and to re-analyse the underlining data again. Figure 5 shows the results of this transformation. For calculation of appropriate linear regression functions, five independent data sets ranging over various spatial scales were incorporated (cf. Euler & Herget 2011, 2012). The newly derived analytical models can now be applied for direct determination of tip and mean flow velocities. They offer the

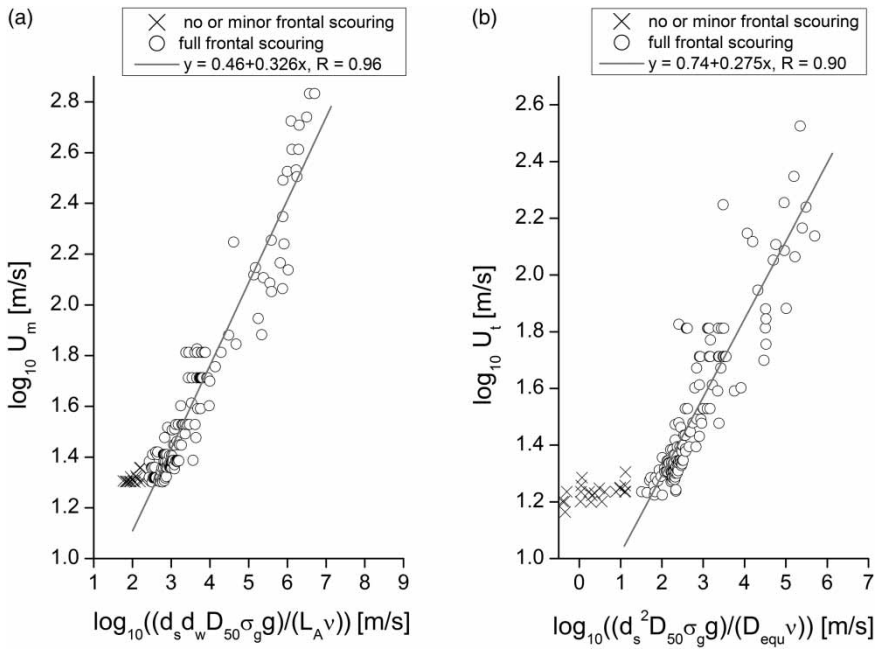

Figure 5 | Re-analysis of the scour data used for analytical model derivation in Euler & Herget (2011, 2012). U_m = mean flow velocity, U_t = tip-velocity, d_s = frontal scour depth, d_w = water depth, D_{50} = median of the grain size distribution, σ_g = geometric standard deviation of the grain size distribution $((D_{84}/D_{16})^{1/2})$, g = gravitational acceleration, L_A = equivalent length of projected frontal area $(h_o^{2/3}\, w_o^{1/3})$, ν = kinematic viscosity, D_{equ} = equivalent diameter of projected frontal area $(2((h_o\, w_o)/\pi)^{1/2})$, w_o = obstacle width, h_o = obstacle height. The data sets comprise own experimental laboratory data which have been added to by laboratory data from Dey *et al.* (2008), prototype-scale experimental data by Sheppard *et al*. (2004) and field bridge scour data provided by the US Geological Survey. In (a), scour depth data recently surveyed in two Spanish ephemeral streams (Euler 2012) were additionally integrated. Unfortunately, no information on tip-velocities could be determined here, so that incorporation of these data into (b) was not possible. The values in both diagrams are plotted as decadic logarithms to account for the large range of spatial scales. It becomes obvious that the performance of the regression function in (a) is more significant compared with the regression function in (b) and thus more suitable for flow reconstruction. On the other hand, the model derived from (b) contains only one flow variable (U_t) compared with two (U_m and d_w) in the first model (a).

advantage that they do not depend on empirical correction factors for sediment size, but use absolute values, instead. Also, the flow velocities can be estimated directly now:

$$\log_{10}(U_m) = 0.46 + 0.326 \log_{10}\left(\frac{d_s\, d_w\, D_{50}\, \sigma_g\, g}{L_A\, \nu}\right) \quad (6)$$

$$\log_{10}(U_t) = 0.74 + 0.275 \log_{10}\left(\frac{d_s^2\, D_{50}\, \sigma_g\, g}{D_{equ}\, \nu}\right) \quad (7)$$

After successful flow reconstruction, ideally the results are verified using data from different palaeohydraulic studies in the same region. This verification also helps to reduce ranges of uncertainties and to adjust the calculated results.

OBSTACLE MARKS BY PLEISTOCENE MEGAFLOODS

From both of the Pleistocene glacial lake outburst floods from Lake Missoula and in the Altai Mountains mentioned in the introduction, several large-scale obstacle marks are identified. The locations, the conditions of the obstacle marks and their position in the outburst flood environments are described below in review, while the most relevant data for the palaeohydraulic interpretation are compiled in Table 2.

Rocky Butte

Rocky Butte is a bedrock hill of volcanic origin in the eastern part of the city of Portland, Oregon, located in the pathway of the repeated outburst floods from Lake Missoula in the Columbia River valley (Bretz 1925, 1969).

The scour in front of Rocky Butte is well developed with frontal scour extending over the entire width of the hill and a tail of deposited sediments in the wake. Only the lateral scour parts are less developed. According to our own surveys and the analysis of satellite images and digital elevation models, the depth of the scour hole is about 33 m, its width 1,750 m and length 290 m. Due to the roads, railway track and settlements, the detailed topography is less certain, but might be less important due to the scale of the entire feature (Figure 6). According to the

Table 2 | Main parameters of Pleistocene obstacle marks and estimated flow velocities

Parameter	Rocky Butte	Chagan Uzun	Boulder near Inya
w_o = obstacle width	1,680 m	330 m	10.8 m
h_o = obstacle height	30–58 m	(a) 23 m (not submerged)	3.1 m
		(b) 40 m (submerged)	
D_{50} = median of the grain size distribution	~0.2 m	0.044 m	0.014 m
σ_g = geometric standard deviation of the grain size distribution ($(D_{84}/D_{16})^{1/2}$)	(=1.0)	2.88	2.61
d_w = water depth	30–58 m (not submerged)	(a) 23 m (not submerged)	6–12 m (submerged)
		(b) < 360 m (submerged)	
d_s = scour depth	33 m	9 m	>2.27 m
d_{s_pot} = potential scour depth[a]	90 m	35 m	2.3 m
w_s = scour width	1,750 m	340 m	24.3 m
l_s = scour length	250–400 m	92 m	6 m
w_r = width of ridge	1,700 m	–	~11 m
U_m = mean flow velocity	6.8–7.3 m/s	(a) 4.4 m/s	2.8–3.5 m/s
		(b) 9.6 m/s	
U_t = tip velocity	4.1–4.5 m/s	(a) 2.5 m/s	1.8 m/s
		(b) 2.35 m/s	

[a]Estimations of potential scour depths are based on the empirical relationships of the scour hole geometry at steady-state conditions.

Figure 6 | Photograph and principal obstacle mark configuration at Rocky Butte, Portland. In the schematic obstacle mark configuration, the small arrow illustrates the perspective of the view of the photo. The black area marks the shape of the obstacle while the eroded scour hole marked by '−' is limited by an escarp signature at its border line. The principal configuration of the ridge in the wake is marked by '+' in addition to the stippled pattern. Scale for principal dimensions.

empirical relationships of scour hole geometry (Figure 4), the depth of the scour should have reached about 90 m. The reason for the limited developed might be seen in the limited thickness of an erodible sediment cover above the frontal roots of the volcanic hill rather than a post-flood refill of 60 m. A missing strength of the downflow current and horseshoe vortex during the final stage of a flood might be considered as reason for a significant fill of the scour hole by gravity sliding. In the wake, the deposits form ridges of nearly 3 km length in the north parallel to the contemporary Columbia River valley and more than 1 km in the south (Allen & Burns 1986).

Rocky Butte itself has a frontal width of 1,680 m. The current top of the hill itself has an altitude of about 185 m asl (above sea level) while the mean level around it is at an elevation of around 92 m asl. The frontal slope shows an average mean inclination of 32°, which is still above the critical values for its full development of the horseshoe vortex system according to preliminary flume experiments by Zemke (2011).

Outburst flood deposits in the area are characterised by boulders up to 0.75–1.0 m and cobbles, which are hosted in a pebbly sand matrix (Peterson *et al.* 2011), hence the characteristic sediment grain size should be less than the boulder size. Unfortunately, exact data on grain size distributions are not available here. Based on the given characteristic boulder size and a photograph (Peterson *et al.* 2011, Figure 7 therein) a probable representative grain size in the magnitude of 0.2 m might be considered as the representative value.

The maximum water level in the area during the outburst floods was 122 m asl, in the locality of Rocky Butte it is assumed it reached up to approximately 150 m asl – hence, Rocky Butte was not submerged (Minervini *et al.* 2003).

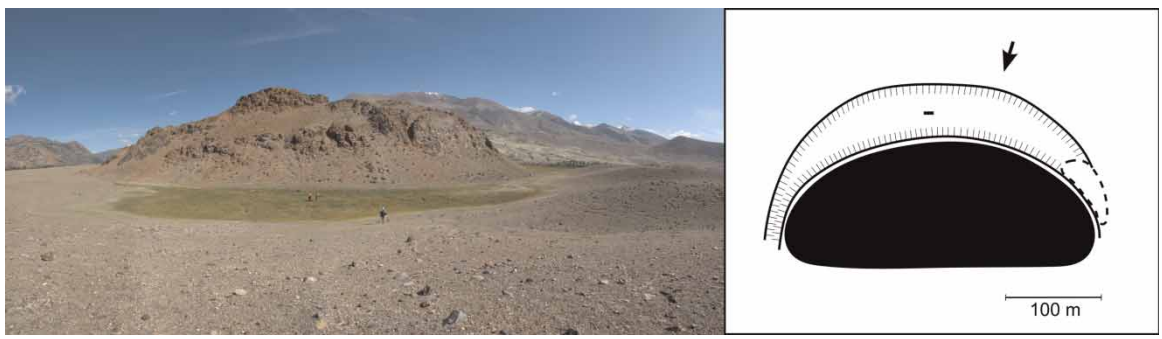

Figure 7 | Photograph and principal obstacle mark configuration at Chagan Uzun, Altai Mountains, Siberia. The small arrow in the obstacle mark sketch illustrates the perspective of view of the photo (for further details cf. Figure 6).

The water level of 122 m asl is based on numerous palaeostage indicators in the area and improves previous findings indicating a level of only 105 m asl (Benito 1997). According to the mean reference surface level around Rocky Butte of 92 m asl and an elevation of the mean maximum water level of 122 m asl, mean maximum depth of flow was about 30 m. The 150 m asl water level is an estimation for the magnitude of the local risen water level of about 28 m due to the transfer of kinetic into potential energy in front of the obstacle. This run-up effect might be useful for a plausibility test. Even though Rocky Butte itself is higher, the inundated height was 30–58 m.

Due to the low level of the Pacific Ocean downstream of the Columbia River, the valley incised down to a level of −70 to −75 m during the final stages of the Missoula floods (Peterson *et al.* 2011). The deep incised valley directly next to the obstacle mark might have influenced its shape by local erosion, even if no indicators for such activity are found. Rocky Butte is located in a regional widening of the Columbia valley. The flood spread out with a related decrease in flow velocity indicated by the decreasing grain size of flood deposits along the Portland Delta area according to the distance of the main channel (Minervini *et al.* 2003).

Based on the data above, mean velocity can be estimated as 6.8–7.3 m/s, while tip velocity is in the range of 4.1–4.5 m/s, depending on the volume of the probable elevated water level in front of Rocky Butte.

Flow velocity in the widening area of the Portland Delta must be less than in the comparable narrow valley of the Columbia River upstream. By water level modelling based on HEC-2, Benito (1997) estimated mean flow velocities of nearly 20 m/s at the downstream end of the Columbia Valley and about 8 m/s for the Portland area during peak discharge. As the obstacle mark's dimension represents a stage during the still rising flood, the estimate of slightly lower flow velocities are plausible.

Based on the run-up effect of the locally elevated water level in front of Rocky Butte, flow velocities can be estimated based on the energy transfer from kinetic to potential energy (Herget 2005). Based on the energy equation after Bernoulli, the relationship between mean flow velocity v_m and the difference of the undisturbed and elevated water level Δh (150 m − 122 m = 28 m) is given as $v_m = (g\ \Delta h)^{1/2}$ for a uniform distributed flow velocity. The estimated mean flow velocity of 16 m/s is a maximum value based on the maximum rise of the water level during peak discharge. Note that the hydraulic interpretation of the obstacle mark geometry is related to an unspecific stage during the rising flood, hence a lower flow velocity. As no evidence for the volume of the rise of the water level is found and the value of 150 m is only an assumption by Minervini *et al.* (2003), a more precise value for the maximum upper limit of the flow velocity cannot be given. Assuming in reverse that the mean flow velocity is estimated in a reliable magnitude of about 7 m/s, the water level might have risen only about 5 m in front of Rocky Butte.

Chagan Uzun

Near the village of Chagan Uzun in the western part of Chuja Basin in the Altai Mountains, an obstacle mark was formed near a bedrock outcrop hill. The feature was generated within the previous lake area. Therefore, it cannot be related to peak discharge of the outburst flood but to a local current within the lake basin at an uncertain stage during its drainage.

The obstacle mark shows a classical pattern of a central frontal scour hole with the deepest parts of 9 m in its centre (Figure 7). Potential maximum scour depth is in the magnitude of 35 m for steady-state conditions. This depth is not preserved as sliding into the frontal scour hole might have filled parts during the decreasing flood. Preliminary geoelectric investigation excludes interpretations of a shallow sedimentary cover as interpretation for limited development of scour depth (Krautblatter, written communication 2010). According to surveys undertaken by the authors, the length of the scour hole is up to 91.5 m while the width is at least >340 m. The missing detailed value for the scour width is caused by sedimentary filling at one margin resulting in an asymmetric scour hole. At the same section, parts of the outer scour hole's margin failed after the flood and filled parts of the depression by a small slide. Unfortunately, there is no sedimentary deposition left in the wake of the obstacle due to post-flood erosion by the Chuja River.

The obstacle itself consists of a bedrock outcrop of metamorphic quartzite. At the peak, the hill is about 40 m above the surrounding relief with a width of 330 m and a mean frontal inclination of 33°. Even though there is a cover of

weathered rock debris around the bedrock hill, a closer examination indicates that its thickness is negligible in relation to the size of the entire feature.

Grain size analysis of the sediments revealed median diameter $D_{50} = 44$ mm and standard deviation $\sigma_g = 2.88$ (Herget 2005). Frequently, larger clasts of up to 130 mm are found forming a weakly developed armouring layer on the surface of the scour hole, while boulders of a mean diameter of about 0.6 m were probably not transported during the obstacle mark's formation.

Palaeostage indicators directly related to the obstacle mark formation could not be identified. Maximum depth of flow is related to the elevation of the water level during the maximum stage of the ice-dammed lake of 2,100 m asl (Herget 2005), resulting in a local maximum depth of flow of about 365 m. Next to the location of the obstacle mark, fluvial gravel dunes generated during drainage of the lake are located. They are generated in the main current towards the valley outlet from the basin while the obstacle mark is formed next to the area of the obviously highest flow velocity. The dunes are supposed to be antidunes, indicating temporary supercritical flow conditions (Carling *et al.* 2002; Herget 2005). Based on their supposed antidune character and considering the water surface level therefore was more or less parallel to the surface of the bedforms, height of the dunes of up to 23 m (Herget 2005) gives a magnitude of the local depth of flow during the dune formation. Even if the gravel dunes were formed under subcritical flow conditions, an upper limit for the depth of flow for a critical shear stress at the bottom of the lake to move the gravels a maximum of tens of metres is indicated by the bedforms. Additionally, the assumption of simultaneous formation of the antidunes and the obstacle mark is necessary.

During the obstacle mark's formation, bedforms were moving on or next to the obstacle. The vortex system in the frontal part was strong enough to generate the scour hole, while at the margin the volume of the transported sediments did not allow scour formation. As mentioned earlier, some minor parts of the scour hole's margin became weak later on due to a small local slide of parts of the wall.

Based on a flow depth of 23 m, a mean and tip velocity of 4.4 and 2.5 m/s, respectively, can be estimated. As no alternative indicator for depth of flow at the obstacle location could be found, the value of mean flow velocity of 9.6 m/s for maximum water depth (=maximum lake depth) of up to 360 m is a more theoretical value for the uppermost range of flow velocity. In this context it should be considered, that no significant current might be expected to be generated at the lake bottom due to the hyperbolic vertical velocity distribution and especially lake drainage conditions (e.g., Zech *et al.* 2008). Note that the related tip velocity of 2.35 m/s is very close to the value of a significantly lower water depth.

Further plausibility tests can be based on different aspects. For the mean flow velocity of 4.4 m/s at a depth of 23 m, a Froude number of 0.3 can be calculated. As the value for the depth of flow is based on the assumed supercritical antidune character of the nearby bedforms, the low Froude number does not fit perfectly. On the other hand, the obstacle is located approximately 1 km from the main palaeocurrent connecting the best-developed antidune crests with the outlet channel of Chuya Basin (Herget 2005). A lateral change of current conditions from >15 m/s (for $Fr = 1$) at the thalweg to ~4 m/s in the locally widening cross-section area is within the range of plausible magnitudes considering supercritical flow.

Boulder near Inya

In the Altai Mountains near the village of Inya, the Pleistocene outburst floods directed through Katun River valley formed an obstacle mark at a boulder. The boulder was also deposited there during an earlier stage of one of the outburst flood events.

The typical and completely developed obstacle mark became visible through an artificial ditch exposing parts of the frontal and lateral scour hole (Figure 8). Even though the scour hole became filled by post-flood loess deposits, its dimensions are clearly visible by topography and changes in vegetation cover. According to the geodetic survey documented in detail in Herget (2005), the width of the scour hole extending on both sides along the boulder is 24.3 m with a frontal depth of at least 2.27 m. A gravel hump of reworked gravels from the scour hole is located approximately 5 m downstream of the boulder and reaches a height of up to 0.50 m above the surrounding surface. Its width of about 11 m is only an approximate value as the hump fades out laterally.

Figure 8 | Photograph and principal obstacle mark configuration at a boulder near Inya, Katun River valley, Altai Mountains, Siberia. The small arrow in the obstacle mark sketch illustrates the perspective of view of the photo (for further details cf. Figure 6).

The obstacle is a streamlined boulder with a width of 10.8 m, length of 13.8 m and height of 3.1 m. The mean frontal inclination is about 27°. According to a weak keel line on the boulder's surface, Herget (2005) argued for a change of the main current direction related to the lateral extension of the giant bar downstream of the boulder (Figure 8). More plausible could be a rotational component of the movement of the boulder into the frontal scour hole during peak formative flow conditions, which is obvious as the frontal part of the boulder is located deep inside the scour hole. It should be noted that the above postulated threshold for tilting ($d_s = 0.6\ l_o$) may likely vary with asymmetric obstacle shapes and uneven internal weight distributions.

Analysis of the local sediments reveals values of $D_{50} =$ 14 mm, $\sigma_g = 2.61$, while the largest clasts in the sediments surrounding the boulder have a mean diameter of about 60 mm (Herget 2005).

Unfortunately, there is no palaeostage indicator without some degree of uncertainty available for an estimation of the depth of flow during the obstacle mark's formation. As the boulder must have been deposited before the initiation of the local scouring, maximum depth of flow (approximately 230 m) related to peak discharge is definitely an overestimation. Assuming a lower value, e.g., termination of the lateral extension of the giant bar by taking the elevation of the sharp edge of the bar as a depth indicator (approximately 45 m) is purely arbitrary. Downstream of the obstacle, fluvial gravel dunes developed at the same level as the obstacle mark. Taking this as an indicator for simultaneous formation, the characteristic range of the depth of flow for the formation of the gravel dunes according to their size of 6–12 m (Herget 2005) might also be considered for the location of the obstacle mark.

Even though the scour hole was later filled up by loess deposits, the contours of the obstacle mark are obvious. Closer inspection indicates that the depth of the scour is only a minimum value based on the visible thickness of the loess deposit. According to the empirical relationship of scour geometry (Figure 4), the value of potential scour depth of 2.3 m indicates that steady-state conditions were reached and still are preserved for this example.

Based on the depth of flow of 6–12 m, a mean velocity between 2.8 m/s and 3.5 m/s and a tip velocity of 1.8 m/s can be estimated.

For plausibility, the estimations for flow velocity might be compared with the values determined for the formation of the gravel dunes downstream. Considering the narrowing valley downstream from approximately 1,350 m for a depth of flow of 10 m at the boulder to 920 m at the gravel dunes, the higher mean flow velocity of ~7 m/s at the gravel dunes (Herget 2005) to 3.5 m/s at the boulder can partly be explained. Note that the estimation of mean flow velocities for the formation of the gravel dunes is just an indicator of a plausible magnitude.

DISCUSSION

This work represents a new approach in palaeohydrology, as it is the first time quantitative hydraulic interpretation of obstacle marks has been applied to palaeoflood

reconstruction. In the context of Pleistocene megafloods, these features have been described and analysed before (e.g., Bretz 1925, 1969; Baker 1973, 1978; Allen & Burns 1986; Herget 2005), but not quantitatively interpreted in the hydraulic context due to limited experience. The developed approach requires detailed understanding of the relevant processes to determine the required parameters from field evidence and plausible reliable estimations if not all parameters can be derived directly. The main advantage of the approach is its independence of obvious problems for upscaling for the application on megafloods. Even though this possibility cannot be proven empirically on megafloods, the linear relationship from flume experiments to the regular flood scale is obvious. The regression coefficients of up to 1.00 indicate a physical and functional context for upscaling over more than two magnitudes, scour holes from centimetres to several metres (Figure 4). A further extrapolation of megafloods appears unnecessary due to the positive experiences presented and in similar cases. From the perspective of fluid mechanics, the similarity of the current pattern around obstacles in flowing water with vortex streets in the atmosphere, is obvious. For example Young & Zawislak (2006) document the obvious relationship of pattern and dimensions for upscaling this phenomenon over several magnitudes from laboratory studies to the wind pattern in the wake of mountains and islands. Bias is only caused by gaps in the basic theory and consequences of unsteady flow conditions. At the current state of knowledge, there is no obvious reason for not assuming the realistic perspective for upscaling knowledge on obstacle marks from flume and recent field studies to Pleistocene megafloods. As mentioned in the Introduction, other approaches such as the interpretation of transport competence have significant limitations for upscaling beyond thresholds (e.g., grain size >0.3–1 m).

The approach is rather sensitive on data for grain size, depth of flow and scour depth. Giving representative data for grain size in relatively coarse materials is a classical problem of representative sampling and the consideration of spatial variability. Sensitivity tests by plausible ranges of representative grain sizes support reliable estimations.

For the estimation of the mean flow velocity, depth of flow at the obstacle must be given, which could be challenging for palaeofloods. Also for not submerged obstacles, this parameter must be quantified for the calculation of the equivalent length L_A and diameter of the projected frontal area D_{equ} based on the dimensions of the obstacle (Equations (6) and (7)). The overestimation of the run-up effect at Rocky Butte illustrates consequences of uncertainties. Closer examination identifies that the main problem is that the left-over obstacle mark dimension is not related to peak discharge while typically only this value can be interpreted from palaoestage indicators. During analysis it should be carefully checked whether maximum values can be estimated only while the obstacle mark itself represents a lower discharge regime than peak discharge.

As perfectly illustrated by the example of the obstacle mark at the boulder near Inya, a post-flood refill of the frontal scour hole could hinder the correct consideration of scour depth. For megafloods, scour holes of significant depth should be estimated while depths of 30 m are not extreme values (cf. Table 2). The significant correlations of the parameters of the scour geometries (Figure 4) allow estimations if significant underdevelopments took place. One reason might be gravitated refill of the overdeepened hole or accumulation of post-flood sediments. Especially for megafloods with related large-scale forms, a limited vertical or lateral extension of reworkable sediments above solid bedrock might limit the development of the frontal scour significantly.

One example for the initial development of a Pleistocene obstacle mark is shown at Locust Hill near Plains, western Montana, a location within the previous lake area of Glacial Lake Missoula. During the drainage of the lake, water was flowing through the now dry valley west of Rainbow Lake Pass, passing Locust Hill on both sides (Pardee 1942). Due to its location, palaeohydraulic interpretation of the obstacle mark deals with a local current within the previous lake basin, not the high-magnitude outburst flood itself. At the eastern flank of Locust Hill, five lakes are located, some named due to their characteristic shape Banana Lake (Figure 9). Based on the configuration around Locust Hill, the lakes obviously represent an initial stage of a frontal scour hole starting to develop at the edges of the obstacle. They are incised up to 5 m into bedrock, rather close to the surface below a relatively thin sedimentary and soil cover. Structural elements like local quartz veins and petrological irregularities might influence the separation of the five lake basins. Consequently, no

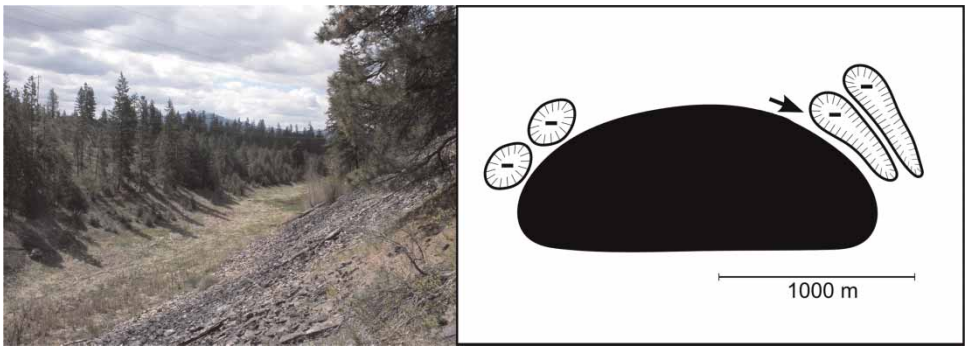

Figure 9 | Photograph and principal obstacle mark configuration at Locust Hill with Banana Lake near Plains, Montana. The small arrow in the obstacle mark sketch illustrates the perspective of view of the photo (for further details cf. Figure 6).

representative grain size of reworked sediments can be determined. The coarse Pleistocene gravels mapped by Pardee (1942) are located more upstream and lateral from the obstacle mark, while the area between the lakes is characterised as denuded rock ledges. The mean inclination of the slopes of Locust Hill of about 9.5° are significantly below the threshold for the development of a significant downflow at the stoss slope of the hill during a lake drainage event. This supports the observation of only laterally initiated incision while a characteristic frontal scour hole is missing.

It should be noted, that here only the classical obstacle mark pattern with a frontal scour hole and a ridge of reworked sediments in the wake is analysed hydraulically. Also from Pleistocene megafloods, additional obstacle mark patterns are found. East of the town of Ephrata, Washington, an obstacle mark was generated by the outburst floods from Lake Missoula. The location within Lower Grant Coulee, one of the characteristic drainage channels of the Channelled Scabland of eastern Washington, was first described and surveyed by Baker (1973). The frontal scour hole is weakly developed while in the wake of the obstacle a scoured depression with a depth of 2.4 m, width of 58 m and length of 118 m was formed (Figure 10). An obvious deposited ridge is missing, but there are weak developed ridges in front and at the lateral parts of the downstream scour hole visible. The boulder has a frontal inclination of 29°, which is still relatively steep, but the obstacle mark has a significantly different pattern. Probably, there was a rather intensive bedload transport of the blocks

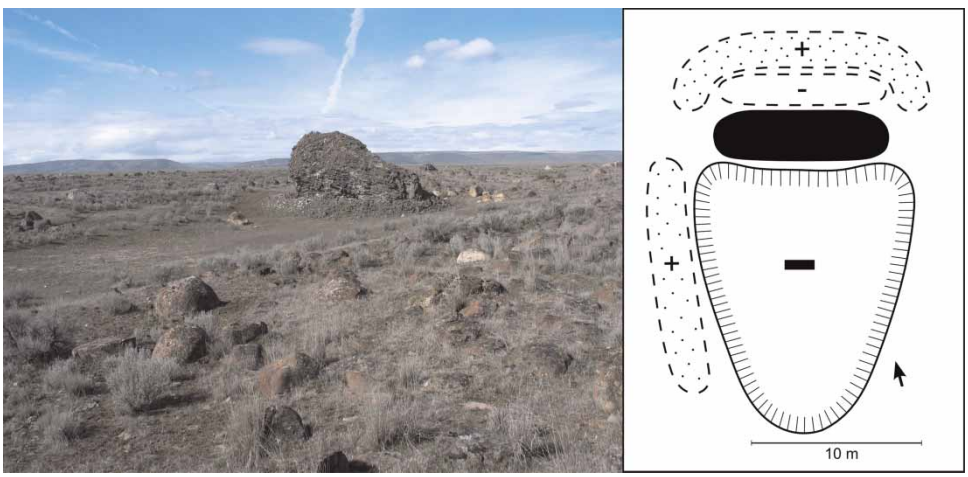

Figure 10 | Photograph and principal obstacle mark configuration at a boulder east of Ephrata, Washington. The small arrow in the obstacle mark sketch illustrates the perspective of view of the photo (for further details cf. Figure 6).

with a mean diameter of 0.5–1 m deposited around the boulder (Figure 8, front) while the lee vortex system generated by the submerged boulder hinders their accumulation in the boulder's wake. Even though no quantitative arguments can be made based on evidence at the location, a suspension transport of the blocks seems less realistic. With the knowledge and experiences reached until now, this pattern cannot be interpreted further in the palaoehydrological context.

Finally, it should be noted that the approach presented here is applied on Pleistocene large-scale obstacle marks. Even though several new findings of such megafloods occur later (e.g., Margold *et al.* 2011), the application to only three examples should not be interpreted as a limitation. Closer examination of the obstacle mark pattern interpreted here can be found frequently wherever water flows, and also allows conclusions on recent current parameters by investigation of the handed-down sedimentary structure.

ACKNOWLEDGEMENTS

The authors appreciate support during field work during recent years by several colleagues; especially mentioned should be Pavel Borodavko (Tomsk), Paul Carling (Southampton), Michael Krautblatter (Bonn), Thomas Neeten (Aachen) and Christiane Thurmann (Bonn). The investigations are financially supported in the framework of different projects by Deutsche Forschungsgemeinschaft DFG (Entstehung und Dynamik fluvialer Hindernismarken, HE 3006/8–1) and Volkswagenstiftung (Hazard assessment and outburst flood estimation of naturally dammed lakes in Central Asia, I/83755). A previous version of the manuscript was significantly improved by the constructive comments and suggestions of Vic Baker and an anonymous reviewer.

REFERENCES

Alho, P., Baker, V. R. & Smith, L. N. 2010 Paleohydraulic reconstruction of the largest Glacial Lake Missoula draining(s). *Quat. Sci. Rev.* **29**, 3067–3078.

Alho, P., Russell, A. J., Carrivick, J. L. & Käyhkö, J. 2005 Reconstruction of the largest Holocene jökulhlaup within Jokulsá á Fjöllum, NE Iceland. *Quat. Sci. Rev.* **24**, 2319–2334.

Alho, P., Roberts, M. & Käyhkö, J. 2007 Estimating the inundation area of a massive, hypothetic jökulhlaup from northwest Vatnajökull, Iceland. *Nat. Hazards* **41**, 21–42.

Allen, J. R. L. 1968 *Current Ripples – Their Relation to Patterns of Water and Sediment Motion*. North Holland Publishing, Amsterdam.

Allen, J. R. L. 1984 *Sedimentary Structures – Their Character and Physical Basis*. Elsevier, Amsterdam.

Allen, J. E. & Burns, M. 1986 *Cataclysms of the Columbia*. Timber Press, Portland, OR.

Baker, V. R. 1973 *Paleohydrology and Sedimentology of Lake Missoula Flooding in Eastern Washington*. Geological Society of America, Special Paper 144, Boulder, CO.

Baker, V. R. 1978 Large-scale erosional and depositional features of the Channeled Scabland. In: *The Channeled Scabland* (V. R. Baker & D. Nummedal, eds), National Aeronautics and Space Administration Planetary Geology Program, Washington, DC, pp. 81–115.

Baker, V. R. 1988 Cataclysmic processes in geomorphological systems. *Z. Geomorphol.* Suppl. **67**, 25–32.

Baker, V. R. 2002 The study of superfloods. *Science* **295**, 2379–2380.

Baker, V. R. 2009 The Channelled Scablands – a retrospective. *Annual Rev. Earth Pl. Sci.* **37**, 393–411.

Baker, V. R., Benito, G. & Rudoy, A. 1993 Paleohydrology of Late Pleistocene superflooding, Altay Mountains, Siberia. *Science* **259**, 348–350.

Benito, G. 1997 Energy expenditure and geomorphic work of the cataclysmic Missoula flooding in the Columbia River gorge, USA. *Earth Surf. Process. Land.* **22**, 457–472.

Bretz, J. H. 1925 The Spokane Flood beyond the Channeled Scablands – part II. *J. Geol.* **33**, 236–259.

Bretz, J. H. 1969 The Lake Missoula floods and the Channeled Scablands. *J. Geol.* **77**, 505–543.

Bridge, J. S. 2003 *Rivers and Floodplains – Forms, Processes, and Sedimentary Record*. Blackwell, Oxford.

Brunner, G. W. 2010 *HEC-RAS River Analysis System User's Manual – Version 4.1*. US Army Corps of Engineers, Davis, CA.

Carling, P. A. 1996a A preliminary palaeohydraulic model applied to late Quaternary gravel dunes – Altai Mountains, Siberia. In: *Global Continental Changes – The Context of Palaeohydrology* (J. Branson, A. G. Brown & K. J. Gregory, eds), Geological Society Special Publication 115, London, pp. 165–179.

Carling, P. A. 1996b Morphology, sedimentology and palaeohydraulic significance of large gravel dunes, Altai Mountains, Siberia. *Sedimentology* **43**, 647–664.

Carling, P. A. 1999 Subaqueous gravel dunes. *J. Sediment. Res.* **69**, 534–545.

Carling, P. A., Kidson, R., Cao, Z. & Herget, J. 2003 Palaeohydraulics of extreme flood events – reality and myths.

In: *Palaeohydrology – Understanding Global Change* (K. J. Gregory & G. Benito, eds), Wiley, Chichester, pp. 325–336.

Carling, P. A., Kirkbride, A. D., Parnachov, S., Borodavko, P. S. & Berger, G. W. 2002 Late Quaternary catastrophic flooding in the Altai Mountains of south-central Siberia – a synoptic overview and a introduction to flood deposit sedimentology. In: *Flood and Megaflood Processes and Deposits: Recent and Ancient Examples* (P. I Martini, V. R. Baker & G. Garzón, eds), Special Publications of the International Association of Sedimentologists 32, Blackwell, Oxford, pp. 283–290.

Carling, P. A., Villanueva, I., Herget, J., Wright, N., Borodavko, P. & Morvan, H. 2010 Unsteady 1D and 2D hydraulic models with ice dam break for Quaternary megaflood, Altai Mountains, southern Siberia. *Global Planet. Change* **70**, 24–34.

Carrivick, J. L., Russell, A. J., Tweed, F. S. & Twigg, D. 2004 Palaeohydrology and sedimentary impacts of jökulhlaups from Kverkfjöll, Iceland. *Sediment. Geol.* **172**, 19–40.

Chang, W.-Y., Lai, J.-S. & Yen, C.-L. 2004 Evolution of scour depth at circular bridge piers. *J. Hydraul. Eng.* **130**, 905–913.

Chow, V. T. 1959 *Open Channel Hydraulics*. McGraw-Hill, New York.

Clarke, G. K. C., Leverington, D. W., Teller, J. T. & Dyke, A. S. 2004 Paleohydraulics of the last outburst flood from glacial Lake Agassiz and the 8200 BP cold event. *Quat. Sci. Rev.* **23**, 389–407.

Clarke, G. K. C., Mathews, W. H. & Pack, R. T. 1984 Outburst floods from glacial Lake Missoula. *Quat. Res.* **22**, 289–299.

Costa, J. E. 1983 Paleohydraulic reconstruction of flash-flood peaks from boulder deposits in the Colorado Front Range. *Geol. Soc. Am. Bull.* **94**, 986–1004.

Denlinger, R. P. & O'Connell, D. R. H. 2010 Simulation of cataclysmic outburst floods from Pleistocene Glacial Lake Missoula. *Geol. Soc. Am. Bull.* **122**, 678–689.

Dey, S, Raikar, R. V. & Roy, A. 2008 Scour at submerged cylindrical obstacles under steady flow. *J. Hydraul. Eng.* **134**, 105–109.

Erlingsson, U. 2008 A jökulhlaup from Laurentian captured ice shelf to the Gulf of Mexico could have caused the Bølling Warming. *Geogr. Ann.* **90A**, 125–140.

Euler, T. & Herget, J. 2011 Obstacle-Reynolds-number based analysis of local scour at submerged cylinders. *J. Hydraul. Res.* **49**, 267–271.

Euler, T. & Herget, J. 2012 Controls on local scour and deposition induced by obstacles in fluvial environments. *Catena* **91**, 35–46.

Euler, T. 2012 *Formation and dynamics of fluvial obstacle marks*. Faculty of Natural Sciences, Bonn, Unpublished Dissertation Thesis.

Fahnestock, R. K. & Haushild, W. L. 1962 Flume studies on the transport of pebbles and cobbles on a sand bed. *Geol. Soc. Am. Bull.* **73**, 1431–1436.

Fay, H. 2002 The formation of ice-block obstacle marks during the November 1996 glacier outburst flood (jökulhlaup), Skeiðarársandur, southern Iceland. In: *Flood and Megaflood Processes and Deposits: Recent and Ancient Examples* (P. I. Martini, V. R. Baker & G. Garzón, eds), Special Publications of the International Association of Sedimentologists 32, Blackwell, Oxford, pp. 85–97.

Herget, J. 2005 *Reconstruction of Pleistocene ice-dammed lake outburst floods in the Altai-Mountains, Siberia*. Geological Society of America Special Publication 386, Boulder, CO, USA.

Howard, D. A., Beach, S. L. & Beach, T. 2011 Field evidence and hydraulic modeling of a large Holocene jökulhlaup at Jökulsá á Fjöllum channel, Iceland. *Geomorphology* **85**, 119–129.

Jarrett, R. D. & England, J. F. 2002 Reliability of paleostage indicators for paleoflood studies. In: *Ancient Floods, Modern Hazards – Principles and Applications of Paleoflood Hydrology* (P. K. House, R. H. Webb, V. R. Baker & D. R. Levish, eds), Water Science and Application 5, American Geophysical Union, Washington, pp. 91–109.

Kehew, A. E., Lord, M. L., Kozlowski, A. L. & Fisher, T. G. 2009 Proglacial megaflooding along the margins of the Laurentide Ice Sheet. In: *Megaflooding on Earth and Mars* (D. M. Burr, P. A. Carling & V. R. Baker, eds), Cambridge University Press, Cambridge, pp. 104–127.

Komar, P. D. 1989 Flow-competence evaluations of the hydraulic parameters of floods – an assessment of the technique. In: *Floods – Hydrological, Sedimentological and Geomorphological Implications* (K. Beven & P. Carling, eds), Wiley, Chichester, pp. 107–134.

Lai, J.-S., Chang, W.-Y. & Yen, C. L. 2009 Maximum local scour depth at bridge piers under unsteady flow. *J. Hydraul. Eng.* **135**, 609–614.

Lee, O. S. & Sturm, T. W. 2009 Effect of sediment size scaling on physical modeling of bridge pier scour. *J. Hydraul. Eng.* **135**, 793–802.

Leeder, M. 1999 *Sedimentology and Sedimentary Basins – From Turbulence to Tectonics*. Blackwell, Malden.

Margold, M., Jansson, K. N., Stroeven, A. P. & Jansen, J. D. 2011 Glacial Lake Vitim, a 3000-km³ outburst flood from Siberia to the Arctic Ocean. *Quat. Res.* **76**, 393–396.

Matthes, G. H. 1947 Macroturbulence in natural streams. *Am. Geophys. Union Trans.* **28/2**, 255–262.

Melville, B. W. & Coleman, S. E. 2000 *Bridge Scour*. Water Resources Publications, Highlands Ranch, CO.

Minervini, J. M., O'Connor, J. E. & Wells, R. E. 2003 Maps showing inundation depths, ice-rafted erratics, and sedimentary facies of late Pleistocene Missoula floods in the Willamette Valley, Oregon. US Geological Survey Open File Report 03–408.

Miyamoto, H., Komatsu, G., Baker, V. R., Dohm, J. M., Ito, K. & Tosaka, H. 2007 Cataclysmic scabland flooding: insights from a simple depth-averaged numerical model. *Environ. Modell. Softw.* **22**, 1400–1408.

Murton, J. B., Bateman, M. D., Dallimore, S. R., Teller, J. T. & Yang, Z. 2010 Identification of Younger Dryas outburst flood path from Lake Agassiz to the Arctic Ocean. *Nature* **464**, 740–743.

Nakayama, K., Fielding, C. R. & Alexander, J. 2002 Variations in character and preservation potential of vegetation-induced

obstacle marks in the variable discharge Burdekin River of north Queensland, Australia. *Sediment. Geol.* **149**, 199–218.

O'Connor, J. E. & Baker, V. R. 1992 Magnitudes and implications of peak discharges from glacial Lake Missoula. *Geol. Soc. Am. Bull.* **104**, 267–279.

O'Connor, J. E., Grant, G. E. & Costa, J. E. 2002 The geology and geography of floods. In: *Ancient Floods, Modern Hazards – Principles and Applications of Paleoflood Hydrology* (P. K. House, R. H. Webb, V. R. Baker & D. R. Levish, eds), Water Science and Application 5, American Geophysical Union, Washington, pp. 359–385.

Oliveto, G. & Hager, W. H. 2005 Further results to time-dependent local scour at bridge elements. *J. Hydraul. Eng.* **131**, 97–105.

Pardee, J. T. 1942 Unusual currents in glacial Lake Missoula, Montana. *Geol. Soc. Am. Bull.* **53**, 1569–1600.

Peterson, C. D., Minor, R., Peterson, G. L. & Gates, E. B. 2011 Pre- and post-Missoula flood geomorphology of the Pre-Holocene ancestral Columbia River valley in the Portland forearc basin, Oregon and Washington, USA. *Geomorphology* **129**, 276–293.

Rayburn, J. A., Cronin, T. M., Franzi, D. A., Knuepfer, P. L. K. & Willard, D. A. 2011 Timing and duration of North American glacial lake discharges and the Younger Dryas climate reversal. *Quat. Res.* **75**, 541–551.

Rudoy, A. N. & Zemtsov, V. A. 2010 Modelling of hydraulic parameters of diluvial floods of the Chuya-Kuray ice-dammed lake in the late Quaternary. *Ice Snow* **109**, 111–118 (in Russian).

Russell, A. J., Roberts, M. J., Fay, H., Marren, P. M., Cassidy, N. J., Tweed, F. S. & Harris, T. 2006 Icelandic jökulhlaup impacts: implications for ice-sheet hydrology, sediment transfer and geomorphology. *Geomorphology* **75**, 33–64.

Sadeque, M. A. F., Rajaratnam, N. & Loewen, M. R. 2008 Flow around cylinders in open channels. *J. Eng. Mech.* **134**, 60–71.

Sengupta, S. 1966 Studies on orientation and imbrication of pebbles with respect to cross-stratification. *J. Sediment. Petrol.* **36**, 362–369.

Sheppard, D. M., Odeh, M. & Glasser, T. 2004 Large-scale clear-water local pier scour experiments. *J. Hydraul. Eng.* **130**, 957–963.

Teller, J. T. 2004 Controls, history, outbursts, and impacts of large late-Quaternary proglacial lakes in North America. In: *The Quaternary Period of the United States* (A. R. Gillespie, S. C. Porter & B. F. Atwater, eds), Elsevier, Amsterdam, pp. 45–62.

Underwood, J. R. & Lambert, W. 1974 Centroclinal cross strata, a distinctive sedimentary structure. *J. Sediment. Petrol.* **44**, 1111–1113.

Young, G. S. & Zawislak, J. 2006 An observational study of vortex spacing in island wake vortex streets. *Mon. Weather Rev.* **134**, 2285–2294.

Zanke, U. 1982 *Grundlagen der Sedimentbewegung*. Springer, Berlin.

Zech, Y., Soares-Frazão, S., Spinewine, B. & Le Grelle, N. 2008 Dam-break induced sediment movement: experimental approaches and numerical modelling. *J. Hydraul. Res.* **46**, 176–190.

Zemke, J. 2011 *Modellierung fluvialer Hindernismarken an geneigten Hindernissen*. Department of Geography, Bonn, Unpublished Diploma Thesis.

First received 31 October 2011; accepted in revised form 6 July 2012. Available online 9 November 2012